© JAN 2026 | IRE Journals | Volume 9 Issue 7 | ISSN: 2456-8880
DOI: https://doi.org/10.64388/IREV9I7-1713852

Sars-Cov-2 Main Protease Inhibition by Bryophyllum Pinatum Phytochemicals: Computational and Kinetics Studies.

IHEANYICHUKWU WOPARA[1], EMERIKE K. KALU[2], STEVE I. OMEODU[3], SHOLA D. OMOSEEYE[4], FELICIA N. OKWAKPAM[5], IDOWU O. OMOTUYI [6]

[1,5]*Department of Biochemistry, Faculty Sciences, Rivers State University, Nkpolu, Nigeria*

[2,3]*Department of Biochemistry, Faculty of Science, University of Port Harcourt, Choba, Nigeria*

[4]*Department of Anatomy, Faculty of Basic Medical Sciences, Ekiti State University, Ado Ekiti, Ekiti State, Nigeria.*

[6]*Department of pharmacology, Faculty of Basic Medical Sciences, Afe Babalola University, Ado Ekiti, Ekiti State, Nigeria*

Abstract

Background: The newly discovered coronavirus infection emerged in Wuhan, China in December 2019 and since then, there has been no FDA approved drugs used in the treatment of corona virus infection, presenting a major challenge to medicine. The protease enzyme in SARS-CoV-2 virus can be a target for the production drugs to manage COVID-19 because of its indispensable role in the replication of the virus.

Results: A total of 102 phytochemicals were identified in Bryophyllum pinnatum any of which could be a potential inhibitor of 3CLpro. These 102 phytochemicals were screened by molecular docking for their binding energies, 3,6-diglucosylapigenin was chosen as lead compound after meeting all the ADMETox qualifications using quikprop software. 3,6-diglucosylapigenin with a binding energy of -10.59Kj/mol shows a good inhibitory activity similar to 3CLpro standard inhibitor; boceprevir. The amino acid interaction between the lead compound and the active site of the protease were examined. MD simulation was performed to analyse Root mean square fluctuation (RMSF), Solvent Accessibility surface area (SASA) and number of hydrogen bond and the results reveled a strong affinity between the 3CLpro and the lead compound. Furthermore, the binding energy of the lead compound was stronger than that of the standard inhibitor. Moreso, the RMSF was decreased at the active site of the enzyme as there was no fluctuation. However, far away from the active site, there was very high fluctuation, opening the active site of the enzyme leading to escape of the ligand.

Conclusions: Ethanolic extract of Bryophyllum pinnatum was used for inhibiting the main protease of SARS-CoV-2 activity with the use of FRET assay to validate the study. Ethanol extracts from Bryophyllum pinnatum at 125.5µg/ml significantly inhibited 3CLpro activity at various concentrations of 100%, 50%, 30%, 10%, 3%, 0.3%, and 0.03%. This study identifies plant phytochemicals that can be a potential agent to combat COVID-19, and can eventually be used for future laboratory and clinical studies.

Index Terms- Sars-cov-2, main protease, Bryophyllum pinatum phytochemicals, RMSF and quikprop

I. INTRODUCTION

Plants have been the primary source of medicinal compounds (drugs) over the years. These plant-based substances are now the building blocks for the synthesis of many synthetic medications. Since then, organic synthesis has advanced significantly, and now, 75% of prescription medications worldwide come from plant sources (Najmi et al., 2022).

The perennial Bryophyllum pinnatum, also known as the "life plant," "love plant," "air plant," and "miracle leaf," is widely used as a traditional medicinal plant in many parts of the world, including China, America, tropical Africa, and India, as part of their medical systems (Kumar et al., 2020). Bryophyllum pinnatum leaf extract has been used as a standard therapy for bacterial, fungal, and viral infections as well as conditions including kidney stones, ulcers, and asthma.Research has unequivocally demonstrated that this plant's leaves are known to have antibacterial and antifungal compounds. Anti-inflammatory, antihypertensive (lowering blood pressure), analgesic, sugar-lowering (anti-diabetic), and even

antimutagenic qualities are all possessed by Bryophyllum pinnatum. B. pinnatum contains active substances such glycosides, flavonoids, bufadienolides, steroids, and organic acids, each of which has been shown to have unique characteristics and functions (Martins et al., 2022). Because B. pinnatum has a wide range of therapeutic action and promise, we planned research to investigate its capacity to inhibit the major protease of SARS-CoV-2. The globe has been dealing with the new coronavirus illness known as COVID-19 since November 2019; its primary symptoms include fever, pneumonia, coughing, nausea, and respiratory failure (Sohrabi et al, 2020).

The cause or etiology of COVID-19 was found to be the severe acute respiratory syndrome coronavirus 2 (SARS-Cov-2). This virus enters the body through the mucous membranes of the upper and lower respiratory tracts and infects other cells, causing a cytokine storm and a series of immune responses (Blanco-melo et al, 2020). For instance, the body's natural killer cells attack body cells that contain the viral RNA and lyse them, releasing the viral RNA into the bloodstream and exposing them to additional immune action. A single-stranded, enveloped positive-sense RNA is called a coronavirus. The largest genome size of the virus, according to published data, is between 26 and 32 kilobases (Chen et al, 2020). Two overlapping polyproteins that are essential for both the transcription and replication of the virus are encoded by a significant portion of this genome, approximately two-thirds of the 5' genome. In a short period of time, the COVID-19 infection turned into a pandemic. As a result of its quick dissemination, the novel human coronavirus, SARS-CoV-2, necessitates the urgent identification of promising targets in the virus for COVID-19 therapy. Repositioning current compounds to treat diseases other than those for which they were initially identified (primary indications) has been an alluring strategy that can expedite the drug discovery process (Altay, *et al*, 2020). Severe Acute Respiratory Syndrome Coronavirus-2 is the official name for the virus that causes COVID-19. Although corona viruses can infect both humans and animals, only human corona viruses are known to cause respiratory infections. The symptoms of Severe Acute Respiratory Syndrome Coronavirus-2 can be mild or severe, ranging from less serious conditions like the common cold to more serious conditions like Middle East Respiratory Syndrome (MERS) and severe acute respiratory syndrome (SARS) (WHO, 2020).

COVID-19 infections can cause symptoms such a cough without phlegm, fever, exhaustion, nausea, vomiting or diarrhea, headache, conjunctivitis, and loss of taste or smell (Weng et al., 2021) From extremely minor or even asymptomatic to severe symptoms or even death, these signs can vary widely. The majority of symptoms typically appear 14 days after exposure and are moderate (Struyf et al., 2022). Other people, meanwhile, can show up with more serious side effects including respiratory failure or pneumonia. The pharmaceutical and medical industries have a significant difficulty in addressing this illness; the development of a successful medication that is target-specific for the treatment of COVID-19 is required (Lai et al., 2020). The polyproteins and distinct parts of the virus's replication mechanism make the SARS-CoV-2 intriguing targets for therapeutic interactions. In 2021, Zakharova et al. COVID-19 patients as well. Numerous highly renowned products have been developed in the battle against COVID-19. A lot of people self-medicate. Additionally, several companies have manufactured and marketed goods that purport to cure COVID-19 (FDA, 2020c). These goods include cannabinol, minerals, vitamins, grape fruit seeds, and more. To combat the coronavirus, drug discovery technology uses computational methods to find small, drug-like compounds that mimic or have strong structural and functional similarities to ligands with high affinity that are powerful non-covalent inhibitors of the main protease of SARS-CoV-2 (Rahman et al., 2022). No research has been done on the kinetics or computation of SARS-COV-2 Main protease inhibition by phytochemicals found in Broyphyllum Pinnatum.

II. MATERIALS AND METHOD

Starting Bio-Systems

Ligand-metribolone complexed with human androgen receptors (R1881) (PBD ID: 1E3G) is the human-androgen receptor coordinate for this study was gotten. (Matias et al., 2000). the 2D structures of cannabinol (CBD) gotten from a public repository or database for chemical substances (PubChem

Compound Identifier: 644019), delta9-Tetrahydrocannabinol/THC (PubChem: Compound Identifier 16078), were docked into the androgen receptor by using the coordinates of (17BETA)-17-HYDROXY-17-METHYLESTRA-4,9,11-TRIEN-3-ONE (R18).

Biosystem Relaxation and Equilibration

At PH of 7.4, all the residues in Apo, Apo+CBD, Apo+R18, Apo+THC were protonated and then prepared for MD simulation (molecular dynamic simulation) at p^H 7.4 and then prepared for Molecular Dynamics (MD) simulation with the use of CHARMM-GUI software (Choi et al., 2021). Protein residues and ligands were parameterized using CHARMM36 force field and CHarmm generalized force field respectively. Using CHARMM TIP3P water model and Na^+/Cl complexes were immersed and neutralized (Boonstra et al., 2016) under periodic bundary condition, caluclations evaluated using Ewald summation, fixing of hydrogen bond was by SHAKE algorithm, atomic motion integration was by temperature and pressure were controlled by thermostat and Barostat from Brendse(Wells et al., 2015; Zakharova et al., 2020)

All biosystems were equiliberated to avoid errors, reatraining measures were put on dense proteins. During the study, runs for production was limited to 100 and data was collected after every 250ps to be used for QC and other analysis. The soft wares for the simulation and analysis were compiles using GPU (GTX-980, GTX680) cards on HP work stations *Mols and Sims*, Ado Ekiti, Ekiti State, Nigeria.

Post-simulation trajectory quality assessment.

Each trajectory was aligned, PBC-wrapped around the protein-ligand complex before data analysis was carried out in order to avoid error. Then convergence of protein-ca root mean square deviations values were checked. After the first 15-20 runs, the root mean square deviation values become stable for wild type while mutant type became stable after 5 run sand remained so until the simulation was done.

Data analysis

In this study, visual molecular dynamics tool was used unless stated otherwise (Huang and MacKerell, 2013). VMD VolMap plugin was used in the calculation of Water density. Root mean square deviation (RMSD) , root mean square fluctuation (RMSF) and distance were calculated using this analysis tools: gmx rmsf, *gmx rms,* and *gmx distance*; they are GROMACS inbuilt analysis tools. The population distribution and line graph were plotted with the help of GRAPH PAD analysis tool, GROMACS tools for high through-put was used for free energy calculation and 3D free energy Landscapes was done by MATHEMATTICA.

The starting structure for the process of molecular docking was the crystal structure of myricetin covalently bound to the main SARS-CoV-2 protease (3CLpro/Mpro, PDB ID: 7B3E) (Kuzikov et al., 2021)

After this, the co-crystallized structure: 3,5,7-TRIHYDROXY-2-(3,4,5-TRIHYDROXYPHENYL)-4H-CHROMEN-4-ONE is called standard ligand (STD). PubChem was the repository used to get information on characterized compounds (http://pubchem.ncbi.nlm.nih.gov) and when a compound is not in the database, they were sketched and cleaned up using Marvin-Sketch (https://chemaxon.com/marvin). conversion of PubChem 2d compounds to 3D was carried out using openbabel (obabel) with MMFF94 forcefield. Autodock Vina was the tool used for molecular docking (Trott and Olson, 2010), and the compounds were ranked and scored using Vina score (Kcal/mol)

In silico ADMETOx:

ADMETox-related properties (QpCACO, QPlogBB, QPPMDCK and QPlogKHSA) were determined using Qikprop program (Schrödinger 2011d) running in normal mode, this is necessary to avoid wastage that occurs when a drug has poor ADMET profile.

Molecular Dynamics Simulation

Biosystems setup for atomistic simulation

The data for molecular dynamic simulation for each biosystem was generated by CHARMM-GUI webserver (www.charmm-gui.org). ParamChem service (https://cgenff.paramchem.org) was used for parametrization as implemented on CHARMM-GUI webserver. CHARMM36 all-atom additive force field parameters was used to define ligand and protein during biosystem build up also, using CHARMM TIP3P water model and Na^+/Cl complexes were immersed and neutralized (Huang

and MacKerell, 2013 and Boonstra et al., 2016). GROMACS (*ver.* 5) software was used to run molecular dynamics simulation (Van Der Spoel et al., 2005) . Berendsen temperature and pressure coupling algorithms as implemented in GROMACS were used to monitor and keep the biosystems at constant pressure and temperature (NPT; 310K, 1 bar) During equilibration. Van der Waals interactions were estimated at 10 Å. Article mesh Ewald (PME) summation scheme was used to compute long-range electrostatic interactions while equation of atomic motion was integrated using the leap-frog algorithm at 2 fs time step for a total time of 50 ns with positional restraints placed on the heavy atoms in all directions. The simulations for production were performed at 100 ns after all atomic restraints were removed. All calculations were performed on Super-Micro workstations (32-E2600 Intel Xeon CPUs, M6000 GPUs Accelerator PCI-E x16 Card/node) situated at Bio-Computing Research Unit (B-cRU), *Mols and Sims*, Ado Ekiti, Ekiti State, Nigeria.

Post-simulation trajectory analysis and MMPBSA calculation.

In this study, visual molecular dynamics tool was used to draw 3D structures unless stated otherwise (Huang et al., 2013). The *g dist* tool inbuilt in GROMACS software was used to calculate distance between atoms. GraphPad-Prism software was used to plot population plots from distance values and line graphd while GROMACS Tool for high-throughput MM-PBSA calculations (*g_mmpbsa*) algorithm was used to calculate binding free energy (Kumari et al., 2014)

Kinetic Studies

Description

Protease activity is measured by the 3-chymotrrypsinlike protease assay kit. The kit has 96 wells and protease tags that has been purified to be used for 100 enzyme reactions (BPS Bioscience, #100707), The protease inhibitor was included for control. The substrate of 3CL Protease Substrate is (DABCYL-KTSAVLQSGFRKME-EDANS), an internally quenched 14-mer fluorogenic (FRET) peptide. When *EDANS* also called 5-((2-Aminoethyl) amino) naphthalene-1-sulfonic acid which is a donor and acceptor (DABCYL) fluorophores are close, energy is released from EDANS. This energy is doused by DABCYL (intact substrate). 3 chymotrypsin-like enzyme acts on the peptide and cleaves the serine glutamine bond giving rise to a fluorescent peptide called SGFRKME-EDANS. The level or intensity of florescence is directly proportional to the activity of 3 chymotrpsin-like enzyme.

Inhibition kinetics

SARS-CoV-2 3-chymotrypsin-like main protease was used in the assessment of *in vitro* Mpro inhibition. (MBP-tagged) assay kit from PS Bioscience (San Diego, CA, USA) was used. Dithiothreitol was used to prepare the buffer for the assay, 3–5 ng/μL was the concentration of the enzyme after dilution, the diluted enzyme, test samples, positive control and blank (buffer) was then introduced into the micro plate that has 96 wells. Preparation of the stock solutions was by the adding of BPN with the 1× assay buffer. BPN solutions were prepared in a stock solution (10 mg/L in DMSO) and then diluted to a final concentration of 10 μg/L (DMSO concentration was no greater than 0.1%). / . The positive control is 3CL Mpro inhibitor at a concentration of 10 μM. The enzyme and the test compound were incubated at 25 degrees Celsius, the substrate solution was added to the well, then optical density at 360nm and 460nm was taken and recorded for each well using SpectraMax M2 plate. The enzyme was incubated with test compounds at room temperature. The reaction was started by adding the substrate solution to each well followed by recording the optical density of each well using a reader at an excitation wavelength of 360 nm and 400nm for 4 hrs. The mean ± standard deviation was obtained after carrying out three replicates using GraphPad Prism9 (GraphPad Software, La Jolla, CA, USA) which was also used obtain graphics and calculate the IC5.

Collection of materials

Fresh leaves of *Bryophyllum pinnatum*, were harvested from pharmacy farm of Afe Babalola University in Aye Community, Ado L.G.A, Ekiti State, Nigeria. The plant was identified by Prof Omotuyi Olaposi of the Department of Pharmaceutical Science, Afe Babalola University.

Preparation of plant extract

© JAN 2026 | IRE Journals | Volume 9 Issue 7 | ISSN: 2456-8880
DOI: https://doi.org/10.64388/IREV9I7-1713852

The fresh leaves of *B.Pinatum* were collected, washed and air-dried at room temperature and then pulverized using an electronic blender. Then 1000g of the pulverized plant sample was macerated in 10 L of distilled water and allowed to extract for 72h. The extract was thereafter filtered using a cheese cloth, followed by filter paper. The obtained extract was concentrated using water bath via evaporation at a temperature of 40^{o}C. The crude extract weighing about 24g, was then stored in small capped plastic container in a deep freezer until use.

III. RESULT AND DISCUSSION

Table 1: The compound with the least binding energy of 10=10.596 was identified as 3,6-diglucosylapigenin from pubchem and was seen to exhibit similar affinity with the known enzyme inhibitor; Boceprevir.

	NAME OF COMPOUND	MOLECULAR FORMULAR	MOLECULAR WEIGHT	DOCKING SCORE
9796792	Letestuianin C	C19H2004	312.4g/mol	-9,142
701722	Zinc 252630703	C21H23N30	333.4g/mol	-9,742
74977439	3,6-diglucosylapigenin	C27H30015	594,5g/mol	-10.596
23325	1-methoxyhydrochioride	C14H14CINO	247.72g/mol	-9,213
323229	1-amino-2-cyanomethlguanidine	C3H7N5	113.12g/mol	-8.867
323213	Methyl-N-phenylcarbamate	C18H18N203	310.3g/mol	-8.319

However, Table 1 shows the name of the compounds, their pubchem ID, their molecular and formular weight as well as their docking score. The compounds, shows a very good binding affinity to the inhibitor. The six phytochemicals were subjected to qikprop analysis of Schrodinger to determine the ADMETOx qualification, 3,6 diglucosyapiginin with binding energy of -10.596kcal/mol was chosen as the lead compound after meeting all the ADMETOx qualifications as shown in Table 3.2

TABLE 2: ADMETox RESULTS SUMMARY FOR LEAD COMPOUNDS

NAME OF COMPOUND	HERG (< -5 bad	CACO (<25-POOR, >50nm/s - GREAT)	QPLOGBB (-3.0-1.2)	QPLOGMDCK (<25nm/s-POOR, >500-GREAT)	QPLOGKhSA -1.5(Low) 1.5(high)	%HUMAN ORAL ABSORPTION	RULE OF 5
Letestuianin C	- 6.005	5.233	- 3.929	894.456	- 1.007	0.000	3
Zinc252630703	- 5.715	17.775	- 3.175	56.783	- 0.841	20.989	2
3,6-diglucosylapigenin	- 7.528	69.877	- 3.679	345.342	- 1.783	84.800	4

1-methoxyhydrochloride	-5.087	18.195	- 2.413	6.510	- 0.346	51.586	0
1-amino-2-cyanomethylguanidine	-4.823	30.491	- 2.226	11.374	- 0.320	57.081	0
Methyl-N-phenylcarbamate	-5.246	45.523	-3.863	800.345	- 1.175	100.000	3

In-silico pharmacokinetic parameters of bryophyllum pinnatum

Due to its effectiveness and affordability, ADMETox modeling has gained a lot of traction in drug discovery and development (Engkvist et al., 2023). Table 2 displays the findings of the ADMETox screening of all 102 Bryophyllum pinnatum phytochemicals, which were derived from Schrodinger's QIKprop.

HERG (HUMAN ETHR-A-GO-GO RELATED GENE)

The protein Kv11.1, the alpha subunit of a potassium ion channel, is encoded by the gene HERG (the human Ether-à-go-go-Related Gene) (KCNH2). Heart problems arise when these genes are inhibited. Since inhibition is now the leading cause of medication withdrawal, this risk is very important for prospective therapeutic candidates, particularly those treating COVID-19, as cardiac complications are common in COVID-19 patients (Ranard et al., 2020). Compounds with QPlogHERG values <-5 are calcium channel blockers, according to the HERG results of the 102 phytochemicals that were extracted from QIKprop. As a result, they are not the best medication choices since they may cause cardiac toxicity. 3,6-diglucosylapigenin, the main molecule found by the docking result, has a QPlogHERG value of -3.963, which is larger than -5, making it an attractive therapeutic candidate. According to Table 2

Prediction of permeation of bryophyllum pinnatum phytochemical

The size, physicochemical characteristics, complex binding, and elimination in the organs, during circulation, at the blood brain barrier, and within the brain fluids all determine a drug's ability to cross the blood brain barrier and affect the nervous system (QPlogBB), intestine (CACO), and kidney (QPPLOGMDCK) (Shahbazi et al., 2016). A collection of methods can be used to minimize toxicity and improve medication delivery and penetration (Abott, 2013).

The permeability of 102 phytochemicals from Bryophyllum pinnatum was predicted in-silico. Ligprep (Version 3.3 Schrodinger, LLC, New York) produced the 3D structures. The 3D descriptors QPPCACO, QPLogBB, and QPPMDCK were then computed using the derived 3D structure and QIKprop. These descriptors can directly represent a molecule's capacity to cross the blood-brain barrier. Figure. 3.2 displays the suggested values of these descriptors for CNS medications with excellent permeability.

Figure 4.2 below displays the computed findings for 102 compounds from Bryophyllum pinnatum. 95% of the compounds had QPPLogBB and QPPMDCK values that fell within the acceptable range, while up to 90% of the tested phytochemicals had QPPCaCO values that did as well.

The majority of the screened phytochemicals, including the lead compound (3,6-diglucosylapigenin), showed strong permeability based on the results of the permeation descriptors above, making them excellent medication candidates.

Lipinski’s rule of five

Lipinski's rule of five, which examines a drug's biochemical characteristics that may affect its absorption and cell membrane penetration, was used to assess the pharmacokinetic profiles of Bryophyllum pinnatum. According to Lipinski's criteria, a compound must meet at least three of the following requirements in order to be considered drug-like: molecular weight <500 Dalton (DA),

© JAN 2026 | IRE Journals | Volume 9 Issue 7 | ISSN: 2456-8880
DOI: https://doi.org/10.64388/IREV9I7-1713852

calculated Octanol water partition coefficient (Log P) (Lipophilicity) <5, multiple hydrogen acceptors <10, and multiple hydrogen bond donors <5 (Doogue et al., 2013)

As seen in Figure 2 above, the pkCSM online prediction platform was utilized to estimate ADMET parameters, water solubility, intestinal absorption, AMES test, total clearance, hepatotoxicity, and the human maximum tolerated dose (Pires et al., 2015). It was also used to compute molecular weight, number of hydrogen donors, number of hydrogen acceptors, octanol water partition coefficient (Log P), and number of rotateable bonds.

MM-PBSA free energy decomposition

Molecular mechanics/Poisson-Boltzmann surface area (MM-PBSA) is widely utilized in free energy prediction due to its accuracy (Wang et al., 2019). The binding free energy of the Mpro-ligand complexes Boceprevir and the phytochemical (3,6 diglucosyapiginin) from Bryophyllum Pinnatum with SARS-COV-2 major protease was determined during the last 50 ns simulated trajectories using MM-PBSA.

Utilizing both polar and non-polar solvation energy, the binding energy was calculated. The following free energies were examined: average binding energy, polar solvation energy, SASA energy, Vander Waals energy, and electrostatic energy (Table 4.3).

The result revealed a free binding energy of Boceprevir to be -80.691kj/mol while the phytochemical from *Bryophyllum Pinnatum* showed a promising binding affinities against SARS-COV-2 Mpro with binding energy of -20.086kj/mol which is potentially prospective as anti-Covid-19 drug. Table 4.3

Table 3: Polar and Non-polar Solvation Energy of Boceprevir and BPN.

	Boceprevir (Kj/mol)	3,6-Diglucosylapigenin (Kj/mol)
Van der Waal energy	-174.547 +/- 27.605	-67.896 +/- 42.307
Electrostatic energy	-17.597 +/- 10.579	-33.114 +/- 26.567
Polar solvation energy	131.355 +/- 19.098	91.105 +/- 79.384
SASA energy	-19.902 +/- 1.985	-10.180 +/- 6.318
Binding energy	-80.691 +/- 22.737	-20.086 +/- 35.180

Table 3, which breaks down the solvation free energy of a solute into four distinct terms (Van der Waal energy, Electrostatic energy, SASA energy, and Binding energy), displays the polar and non-polar solvation energies of Boceprevir and BPN.

Root mean square fluctuation (RMSF)

RMSF of a residue analyzes a particular segment of the protein that is deviating from its mean structure which happens usually because a ligand has interacted with the protein. (Sharma et al., 2021). The

© JAN 2026 | IRE Journals | Volume 9 Issue 7 | ISSN: 2456-8880
DOI: https://doi.org/10.64388/IREV9I7-1713852

average RMSF values of backbones alpha- carbon atom of Mpro unligated (APO) and associated complexes are calculated to see the changing behavior of amino acids of SARS-COV-2 Mpro. This analysis will provide a useful insight regarding the structural fluctuations of different region of protein.

As seen in Figure 1, the stability of the ligand with the test protein was demonstrated by the fact that the RMSF value of the complexes of Mpro, Boceprevir, and 3,6 diglucosylapiginin stayed below 0.4 nm for the majority of Mpro's amino acids.

Nevertheless, a number of variations were also noted in certain Mpro areas in complex with the ligands, which could be because of the ligands' dynamic activity inside the bonding region. In 2021, Sharma et al. In catalysis, amino acid residues from areas with less variations are crucial. This finding suggests that important amino acid residues in 10-80 and 90-210 could have potent interactions with Bryophyllum Pinnatum phytochemicals.

As seen in Figure 1, the stability of the ligand with the test protein was demonstrated by the fact that the RMSF value of the complexes of Mpro, Boceprevir, and 3,6 diglucosylapiginin stayed below 0.4 nm for the majority of Mpro's amino acids.

Nevertheless, a number of variations were also noted in certain Mpro areas in complex with the ligands, which could be because of the ligands' dynamic activity inside the bonding region. In 2021, Sharma et al. In catalysis, amino acid residues from areas with less variations are crucial. This finding suggests that important amino acid residues in 10-80 and 90-210 could have potent interactions with Bryophyllum Pinnatum phytochemicals.

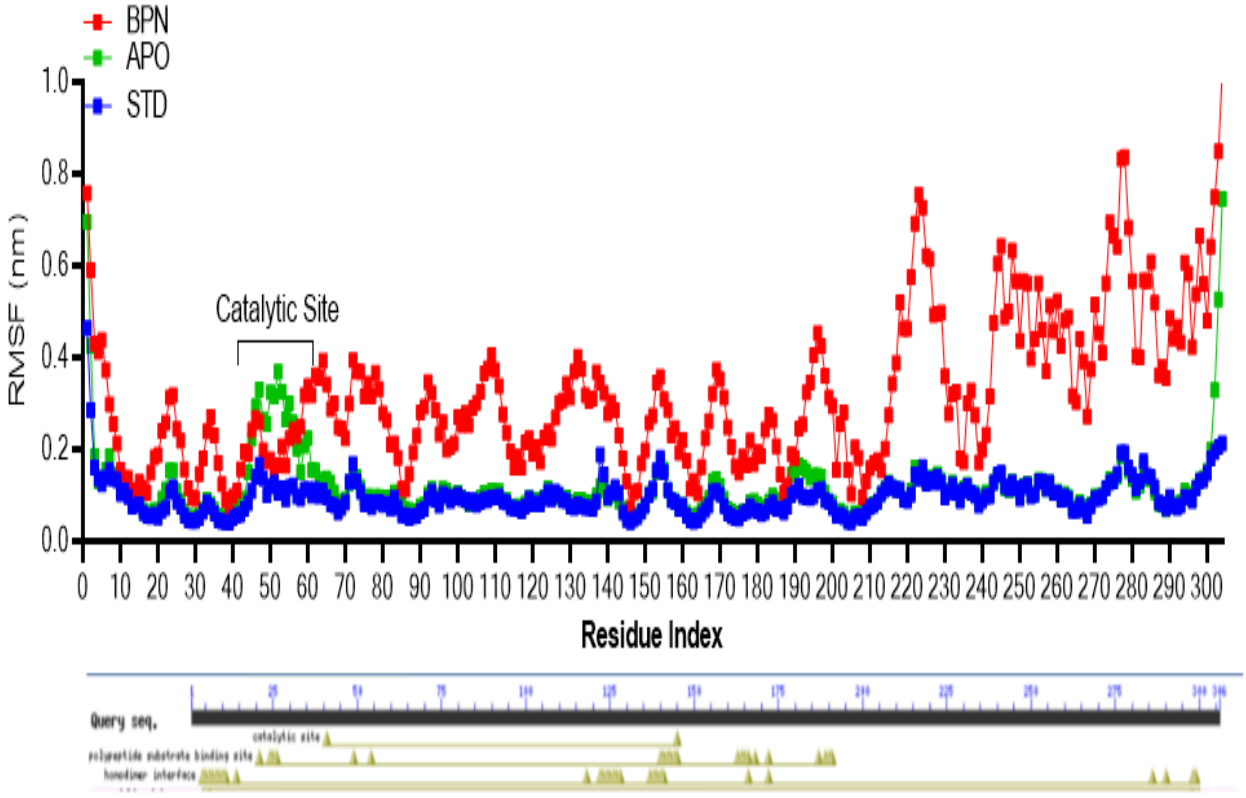

Figure 1: RMSF OF AMINO ACID RESIDUES OF 3CLpro Complexed with LEAD OF BPN and STD.

© JAN 2026 | IRE Journals | Volume 9 Issue 7 | ISSN: 2456-8880
DOI: https://doi.org/10.64388/IREV9I7-1713852

Hydrogen bond numbers analysis

Hydrogen bonding is essential for drugs to bind to the target protein's catalytic region; the quantity of hydrogen bonds that form between protein-ligand complexes plays a significant part in preserving the stability of the enzyme's binding pocket (wang et al., 2017).

The interaction of Mpro with the lead compound 3,6 Diglucosylapiginin from *Bryophyllum Pinnatum* and Boceprevir were studied by calculating the hydrogen bond profiles, the numbers of hydrogen bonds and hydrogen bonds distribution throughout the MD simulation on the scale of 1000ns. As shown in Figure 2

The result revealed that Mpro with the lead compound 3,6 Diglucosylapiginin from *Bryophylulm Pinnatum* phytochemical (RED), form a total of 4 hydrogen bonds for the 1000ns simulation time while the numbers of hydrogen bonds for boceprevir and Mpro indicate 2 throughout the simulation time.

The result showed that the phytochemical 3,6 diglucosylapiginin from *Bryophyllum Pinnatum* was able to maintain a strong interaction with Mpro at the active sites which may be considered as drug candidate for covid-19.

The few numbers of hydrogen bond form with Mpro and Boceprevir may be due to the interaction of water molecules at the binding site of Mpro (wang et al., 2017).

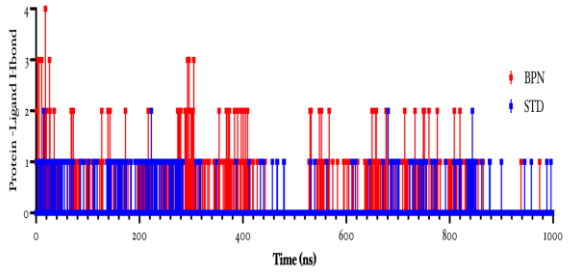

Figure 2: Protein-Ligand Hbond per time of BPN lead and Boceprevir (STD)

Radius of gyration analysis (Rg)

Protein-substrate complex variations in compactness are described by the radius of gyration (Rg). It indicates how a protein folds and unfolds during MD simulation. (Tripathi and Shukla, 2020). We docked the phytochemical 3,6 Diglucosylapiginin from Bryophyllum Pinnatum with the conventional inhibitor (Boceprevir) using the x-ray crystal structure of the newly published SARS-COV-2 Mpro (PDB ID:6ZRU) (Zheng et al., 2020).

To evaluate the structural compactness of SARS-COV-2 Mpro in both the bound state and the APO state (unbound), the virtual structure was put through 1000ns MD simulations using the ligands Boceprevir and 3,6 Diglucosylapiginin phytochemical from Bryophyllum Pinnatum Figure 3**.**

With a high value of Rg of 9.02A, the result indicated that Mpro (unbound) APO is less stiff and compact in its original condition. One possible explanation for this might be that the enzyme is not active in its natural state, which prevents any observable catalysis. The lead compound 3,6 Diglucosylapiginin is a potential inhibitor of SARS-COV2 Mpro and may therefore function as a drug candidate against Covid-19. In contrast, the phytochemical from B.pina with a small value of Rg value of 6.02A indicates that the binding pocket of the enzyme was open in order to accept the ligand for catalysis.

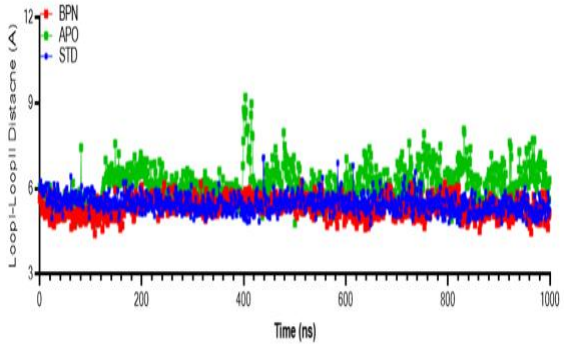

Figure 3: Inter Loop Distance between APO, STD, B.PINA

Active site determination of SARS-COV-2 main protease.

The identification of the potential binding site of drugs on SARS-COV-2 main protease, was performed on the x-ray crystal structure of dimeric Mpro, using the site finder module of molecular operating environment (MOE) (Jin et al., 2020).

© JAN 2026 | IRE Journals | Volume 9 Issue 7 | ISSN: 2456-8880
DOI: https://doi.org/10.64388/IREV9I7-1713852

Based on the MD simulation result as shown in Figure 5, the two critical amino acid residues responsible that contributed to the highest binding energy for the binding activity of Mpro is Cys145 and His 41 and are located in the cleft between domain I (residues 8–101) and domain II (residues 102–184). while figure 4 shows the catalytic domain I and domain II

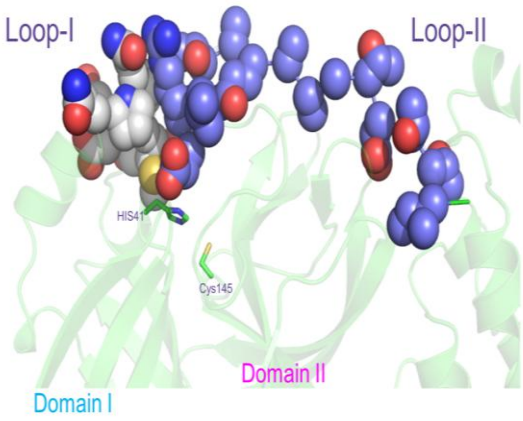

Figure 4: Catalytic site between Domain I and Domain II.

Kinetics assay of SARS-COV-2 inhibitory activity against BPN

Ethanolic extract of *Bryophyllum Pinnatum* was screened for it inhibitory activity against SARS-COV-2 Main protease using FRET assay (FLUOROSENCE RESONANCE ENERGY TRANSFER) at 125.5µg/ml and GC376 as a positive control. The result as shown in Figure 5 revealed the activity of the extract at various concentration of 100, 50, 30, 10, 3, 0.3, 0.03 and 0% respectively. This result demonstrated the ability of the BPN to inhibit the SARS-COV-2 Mpro. By this result it was also observed that bryophylum Pinnatum Extract shows a significant inhibition at the various concentration.

Based on the IC50 of 125.5µg/ml *Bryophyllum Pinnatum* extract indicate a strong inhibitory activity against SARS-COV-2 Mpro and therefore could be a good drug candidate for the treatment of covid-19.

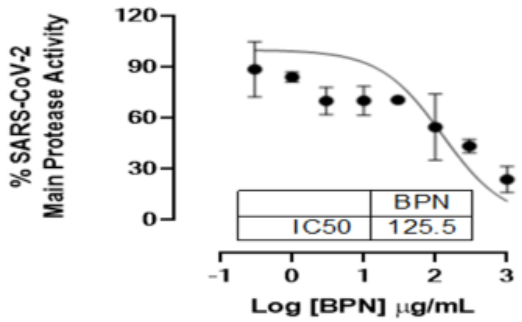

Figure 5: Kinetics Result of *B.pina* Inhibition

The advent of severe acute respiratory syndrome (SARS-COV-2) in 2019 is proof that a highly pathogenic coronavirus has existed in the human population since 2003 (Wang et al, 2020).

When the global death toll hits 5 million and economic losses continue, it is critical to develop drugs that may slow the spread of infection and disease (Wang et al., 2022). The FDA-approved vaccines are now the most effective on the market in the United States, and Remdesivir is licensed to treat hospitalized patients. However, low vaccination rates and the continuous emergence of new virus strains make this study essential.

The 100ns trajectories of the monomeric and dimeric forms of the SARS-COV-2 3CLpro are analyzed in the computational investigation that is being presented here. It is worth noting that the dimeric 3CLpro starting structure used in our simulation was extracted from the PDB: 6ZRU, which had the ligand removed. The results of this work demonstrate that the dimeric form of 3Clpro exhibits distinct conformational dynamics from the monomeric form. Specifically, the monomeric 3Clpro has a more flexible protein chain than the dimeric, and the majority of the protease's flexibility is attributed to the lengthy loops that connect domain I and II. This is also consistent with Zheng et al.'s 2020 in-silico investigation. Show that the substrate binding sites between the cys145-His41 catalytic dyad are more flexible than the 3CLpro monomeric version.

A residue's RMSF examines a specific protein segment that deviates from its mean structure, often as a result of a ligand's interaction with the protein. In 2021, Sharma et al. To see how the amino acids of SARS-COV-2 Mpro change over time, the average RMSF values of

the backbones alpha-carbon atom of Mpro unligated (APO) and related complexes are computed.

The result of the RMSF value of Mpro , Boceprevir and 3,6 diglucosylapiginin complexes remained below 0.4nm for majority of the amino acids of 3CLpro indicating the stability of the ligand with the test protein.

In the present study, the structural stability of the 3CLpro during the simulations, measured the deviation of each structure from the starting crystallographic coordinates after superposition on the protein C & atoms. The RMSF was calculated and plotted. The RMSF provides evidence that all the simulated systems have reached convergent of the structural drift by sampling a local potential energy minimum.

The residue-based root mean square fluctuation (RMSF) in the trajectory was calculated to measure the flexibility of the residues. The data show that the two chains of dimeric protease have different RMSF values in specific regions of the protein.

Specifically, chain A, the first part of the long loop region, residues from 180 to 190, connecting domain II and III, has higher flexibility than chain B.

Our findings are also in agreement with the previous study of Huang et al., 2020 confirming by a combination of experiments and simulations, that the two promoters in the dimer are asymmetric and that only one promoter is active at a time. It is worth noting that the RMSF in monomeric 3Clpro is higher throughout the polypeptide chain as compared with dimeric 3Clpro RMSF, which is lower, especially in the structured regions.

In addition, the RMSF of the loop region from residue 45 to residue 53, is slightly higher than the corresponding region in the monomer and the long loop region, encompassing residues 183 to 193, is higher in the dimeric than monomeric 3Clpro. We speculate a possible correlation of the loop flexibility with interaction of candidate inhibitions.

In addition, this study provide an insight in the intermolecular interactions between the two chains in the dimer, particularly the interactions between the N-terminus and domain III of one monomer, are in turn critical to stabilize the residue of the catalytic pocket in the active form, thus ensuring the successful proceeding of the catalytic cycle in the diner. This further supports that dimerization is important for enzyme activity.

Our findings are also in agreement with previous study by Chen et al., 2020 regarding the 3Clpro of SARS-Cov-2, showing that the right conformation for catalysis in one protomer can be induced upon dimer formation and that the enzyme may follow the association, activation, catalysis, and dissociation mechanism for activity control.

In this study, we found the potential interaction of phytochemicals with the drugable targets of SARS-cov-2 medicated infection in human. For this, we targeted the three key steps of viral pathogenesis namely;

Viral genomic replication, viral precursor conversion to functional proteins (Mpro), and viral entrance into the host cell (spike protein). A crucial stage in the viral entrance into the host cell is the interaction of the protein RBO with the ACE-2 receptor (Senapati et al., 2021). Shang et al. (2020), according to reports, the SARS-Cov-2 S1 domain amino acids 455, 482-486, 493,494, and 501 are crucial for interactions with the human ACE-2 protein. Curenma Longa and Withania somnifera phytochemicals have been shown to have the ability to inhibit the SARS-Cov-2 Mpro protein in silico. The primary chemical that was discovered was visible. In the MD simulation analysis, there was a notable increase in binding capacity at the Mpro active site as compared to conventional inhibitors (Gupta et al., 2010).

The primary chemical 3,6 diglucosylapiginin in Bryophyllum pinnatum interacts with two essential amino acids (Cys 145 and His 41) that are necessary for spike-protein and the human host ACE-2 binding receptor, according to the current study (Gordon et al., 2020).

The lead compound 3,6 diglucosylapiginin (binding efficacy of – 10.598k cal/mol) also showed hydrophobic and hydrogen bond interaction with the key amino acids involved in spike protein domain and ACE-2 protein-protein interaction the result

indicate that 3,6 diglucosylapiginin has the potential to disrupt spike glycoprotein – ACE-2 protein-protein interaction by binding at the SARS-COV-2 RBD. Thus the lead compound might inhibite viral entry into the cell as well decrease Mpro activity, which in turn inhibit the production of functional protein.

It's interesting to note that at different concentrations, ethanolic extracts of Bryophyllum pinnatum leaves significantly decreased SARS-COV-2 3Clpro activity. The polyphenols found in Bryophylllum pinnatum, especially the flavonoids curcumin and its derivatives, are natural substances that have also been taken into consideration in molecular docking studies for their possible ability to inhibit SARS-COV-2 3Clpro (Adem et al., 2020). Although some research suggested that other flavonoids could have better potential inhibitory action based on docking results, Bryophyllum pinnatum can be considered a natural molecule with potential as 3Clpro inhibitors (Souza et al., 2023).

In accordance, our FRET Assay of Bryophyllum pinnatum IC_{50} of 125.5µg/ml at various concentrations revealed a high inhibitory activity against 3Clpro. The BPN extract shows high degree in reduction of 3Clpro viral activities. Thus, the inhibition capacity of Bryophyllum pinnatum might be the result of synergistic activity of several compounds. Overall, our result indicates that extract of BPN are strong candidate for being tested for inhibiting the invivo replication of SARS-Cov-2 and hence a potential drug for Covid-19 treatment.

IV. CONCLUSION

The Corona viruses are a very wide group of viruses that infect humans and other animals. The symptoms of corona virus infection in humans can be mild or severe; mild flu symptoms include flu like symptoms then symptoms progressively become more severe as in cough, fever, loss of taste and smell senses and difficulty in breathing.

This study is aimed at testing the inhibitory effect of *Bryophyllum Pinnatum* phytochemicals against SARS-COV-2 Mpro using a computational as well as in *vitro* kinetics approach. The superimposition of the 3D structures of Mpro provide information on key amino acids involved in the main binding pocket.

This present investigation identified 3,6 diglucosylapiginin as lead compound obtained from *Bryophyllum Pinnatum* in the inhibition of SARS-COV-2 Mpro. Molecular docking study confirmed the binding potential of the phytochemical at the active site of the enzyme (CYS145 and HIS41) residues respectively.

The 3,6 diglucosylapiginin phytochemical from *Bryophyllum Pinnatum* which possess a favorable drug-likeness characteristics with Boceprevir, a known standard inhibitor of SARS-COV-2 Mpro were subjected for 1000ns MD simulations using NAMD, the phytochemical 3,6 diglucosylapiginin had a higher binding energy value than the standard inhibitor boceprevir with a better interaction at the key catalytic residues of Mpro.

The RMSF, SASA energy and Radius of Gyration (Rg) profiles corresponding to 3,6 diglucosyapiginin complexed with Mpro clearly suggest a highly stable and experience less fluctuations. Again the existence of high number of intermolecular hydrogen bonds in the Mpro complexed with the phytochemical from *Bryophyllum Pinnatum* than the Mpro – Boceprevir complex, also suggesting a greater stability of 3,6 diglucosyapiginin in the binding pocket.

This study was further subjected to in *vitro* validation by testing the ethanolic extract of *Bryphyllum Pinnatum* against SARS-COV-2 Mpro using a quenched fluorescence resonance energy transfer (FRET) assay and GC376 as a positive control. The extract from *Bryophyllum Pinnatum* at 125.5µg/ml significantly inhibited 3CLpro activity at various concentrations of 100%, 50%, 30%, 10%, 3%, 0.3%, 0.03% and 0% respectively. This study identifies plant phytochemicals that can be a potential agent for the treatment against COVID-19, acting as a basis for future chemical and in-vivo clinical trials.

V. ACKNOWLEDGEMENTS

We acknowledge the management of the research unit for Molecular Biology and Simulation Center, Ado-Ekiti, Ekiti State, Nigeria, for the provision of the needed facilities for the computer base research.

REFERENCE

[1] Abbott, N. J. (2013). Blood–brain barrier structure and function and the challenges for CNS drug delivery. Journal of inherited metabolic disease, 36, 437-449.

[2] Adem, S., Eyupoglu, V., Sarfraz, I., Rasul, A., & Ali, M. (2020). Identification of potent COVID-19 main protease (Mpro) inhibitors from natural polyphenols: an in silico strategy unveils a hope against CORONA. Preprints, 2020, 2020030333.

[3] Altay, O., Mohammadi, E., Lam, S., Turkez, H., Boren, J., Nielsen, J., ... & Mardinoglu, A. (2020). Current status of COVID-19 therapies and drug repositioning applications. Iscience, 23(7).

[4] Blanco-Melo, D., Nilsson-Payant, B. E., Uhl, S., Escudero-Pèrez, B., Olschewki, S., Thibault, P., ... & tenOever, B. R. (2020). An inability to maintain the ribonucleoprotein genomic structure is responsible for host detection of negative-sense RNA viruses. *bioRxiv*, 2020-03.

[5] Boonstra, A. M., Stewart, R. E., Köke, A. J., Oosterwijk, R. F., Swaan, J. L., Schreurs, K. M., & Schiphorst Preuper, H. R. (2016). Cut-off points for mild, moderate, and severe pain on the numeric rating scale for pain in patients with chronic musculoskeletal pain: variability and influence of sex and catastrophizing. *Frontiers in psychology*, *7*, 1466.

[6] Chen, S., Yang, J., Yang, W., Wang, C., & Bärnighausen, T. (2020). COVID-19 control in China during mass population movements at New Year. The Lancet, 395(10226), 764-766.

[7] Choi, A., Koch, M., Wu, K., Chu, L., Ma, L., Hill, A., ... & Edwards, D. K. (2021). Safety and immunogenicity of SARS-CoV-2 variant mRNA vaccine boosters in healthy adults: an interim analysis. *Nature medicine*, *27*(11), 2025-2031.

[8] Doogue, M. P., & Polasek, T. M. (2013). The ABCD of clinical pharmacokinetics. *Therapeutic advances in drug safety*, *4*(1), 5-7.

[9] Engkvist, O., Mervin, L. H., Chen, H., & Ran, T. (2023). Machine Learning in Drug Design.

[10] FDA. 2020. Fraudulent Coronavirus Disease 2019 (COVID-19) Products.https://www.fda.gov/consumers/health-fraud-scams/fraudulent-coronavirus-...

[11] Gordon, D. E., Jang, G. M., Bouhaddou, M., Xu, J., Obernier, K., White, K. M., ... & Krogan, N. J. (2020). A SARS-CoV-2 protein interaction map reveals targets for drug repurposing. Nature, 583(7816), 459-468.

[12] Gupta, A., Li, P. K. T., Szeto, C. C., Piraino, B., Bernardini, J., Figureueiredo, A. E.,. & Struijk, D. G. (2010). Peritoneal dialysis-related infections recommendations: 2010 update. *Peritoneal Dialysis International*, *30*(4), 393-423.

[13] Huang, J., & MacKerell Jr, A. D. (2013). CHARMM36 all-atom additive protein force field: Validation based on comparison to NMR data. Journal of computational chemistry, 34(25), 2135-2145.

[14] Jin, Z., Du, X., Xu, Y., Deng, Y., Liu, M., Zhao, Y., ... & Yang, H. (2020). Structure of Mpro from SARS-CoV-2 and discovery of its inhibitors. Nature, 582(7811), 289-293.

[15] Kumar, D., Chandel, V., Raj, S., & Rathi, B. (2020). In silico identification of potent FDA approved drugs against Coronavirus COVID-19 main protease: A drug repurposing approach. Chemical Biology Letters, 7(3), 166-175.

[16] Kumar, S., & Saxena, S. K. (2021). Structural and molecular perspectives of SARS-CoV-2. Methods (San Diego, Calif.), 195, 23.

[17] Kumari, R., Kumar, R., Open Source Drug Discovery Consortium, & Lynn, A. (2014). g_mmpbsa□ A GROMACS tool for high-throughput MM-PBSA calculations. Journal of chemical information and modeling, 54(7), 1951-1962.

[18] Kuzikov, M., Morasso, S., Reinshagen, J., Wolf, M., Monaco, V., Cozzolino, F., ... &

Zaliani, A. (2023). Resolving the pharmacological redox-sensitivity of SARS-CoV-2 PLpro in drug repurposing screening enabled identification of the competitive GRL-0617 binding site inhibitor CPI-169. bioRxiv, 2023-10.

[19] Lai, C. C., Liu, Y. H., Wang, C. Y., Wang, Y. H., Hsueh, S. C., Yen, M. Y., ... & Hsueh, P. R. (2020). Asymptomatic carrier state, acute respiratory disease, and pneumonia due to severe acute respiratory syndrome coronavirus 2 (SARS-CoV-2): Facts and myths. Journal of Microbiology, Immunology and Infection, 53(3), 404-412.

[20] Martins Fernandes Pereira K, Calheiros de Carvalho A, André Moura Veiga T, Melgoza A, Bonne Hernández R, Dos Santos Grecco S, Uchiyama Nakamura M, Guo S. The psychoactive effects of Bryophyllum pinnatum (Lam.) Oken leaves in young zebrafish. PLoS One. 2022 Mar 9;17(3):e0264987. doi: 10.1371/journal.pone.0264987. PMID: 35263358; PMCID: PMC8906576.

[21] Matias, P. M., Donner, P., Coelho, R., Thomaz, M., Peixoto, C., Macedo, S., ... & Carrondo, M. A. (2000). Structural evidence for ligand specificity in the binding domain of the human androgen receptor: implications for pathogenic gene mutations. *Journal of Biological Chemistry*, *275*(34), 26164-26171.

[22] Pires, D. E., Blundell, T. L., & Ascher, D. B. (2015). pkCSM: predicting small-molecule pharmacokinetic and toxicity properties using graph-based signatures. Journal of medicinal chemistry, 58(9), 4066-4072.

[23] Rahman, M. M., Islam, M. R., Akash, S., Mim, S. A., Rahaman, M. S., Emran, T. B., ... & Wilairatana, P. (2022). In silico investigation and potential therapeutic approaches of natural products for COVID-19: Computer-aided drug design perspective. Frontiers in Cellular and Infection Microbiology, 12, 929430.

[24] Ranard, L. S., Fried, J. A., Abdalla, M., Anstey, D. E., Givens, R. C., Kumaraiah, D., ... & Masoumi, A. (2020). Approach to acute cardiovascular complications in COVID-19 infection. Circulation: Heart Failure, 13(7), e007220.

[25] Senapati, S., Banerjee, P., Bhagavatula, S., Kushwaha, P. P., & Kumar, S. (2021). Contributions of human ACE2 and TMPRSS2 in determining host–pathogen interaction of COVID-19. Journal of genetics, 100, 1-16.

[26] Shahbazi, S., Sahrawat, T. R., Ray, M., Dash, S., Kar, D., & Singh, S. (2016). Drug targets for cardiovascular-safe anti-inflammatory: In silico rational drug studies. PloS one, 11(6), e0156156.

[27] Shang, J., Ye, G., Shi, K., Wan, Y., Luo, C., Aihara, H., ... & Li, F. (2020). Structural basis of receptor recognition by SARS-CoV-2. Nature, 581(7807), 221-224.

[28] Sharma, A., Bhatt, N. S., St Martin, A., Abid, M. B., Bloomquist, J., Chemaly, R. F., ... & Shah, G. L. (2021). Clinical characteristics and outcomes of COVID-19 in haematopoietic stem-cell transplantation recipients: an observational cohort study. The Lancet Haematology, 8(3), e185-e193.

[29] Sohrabi, C., Alsafi, Z., O'neill, N., Khan, M., Kerwan, A., Al-Jabir, A., ... & Agha, R. (2020). World Health Organization declares global emergency: A review of the 2019 novel coronavirus (COVID-19). *International journal of surgery*, *76*, 71-76.

[30] Souza, M. D. A., Souza, H. C. A., Viana, E. K. A., Alves, S. K. S., Sousa, C. S., Ribeiro, A. S. N., ... & Rocha, J. A. (2023). An In-silico Analysis Study of the Chemical Compounds from the Crassulaceous Plant Bryophyllum pinnatum (Lam.) Oken against the SARS-COV-2 Proteases. Journal of Advances in Medicine and Medical Research, 35(23), 69-91.

[31] Struyf, T., Deeks, J. J., Dinnes, J., Takwoingi, Y., Davenport, C., Leeflang, M. M., ... & Cochrane COVID-19 Diagnostic Test Accuracy Group. (2022). Signs and symptoms to determine if a patient presenting in primary care or hospital outpatient settings has

COVID-19. Cochrane database of systematic reviews, (5).

[32] Trott, O., & Olson, A. J. (2010). AutoDock Vina: improving the speed and accuracy of docking with a new scoring function, efficient optimization, and multithreading. Journal of computational chemistry, 31(2), 455-461.

[33] Van der Spoel, D., van Maaren, P. J., & Caleman, C. (2012). GROMACS molecule & liquid database. Bioinformatics, 28(5), 752-753.

[34] Wang, B., Li, R., Lu, Z., & Huang, Y. (2020). Does comorbidity increase the risk of patients with COVID-19: evidence from meta-analysis. Aging (albany NY), 12(7), 6049.

[35] Wang, Q., Guo, Y., Iketani, S., Nair, M. S., Li, Z., Mohri, H., ... & Ho, D. D. (2022). Antibody evasion by SARS-CoV-2 Omicron subvariants BA. 2.12. 1, BA. 4 and BA. 5. Nature, 608(7923), 603-608.

[36] Wang, Q., Li, B., Xiao, T., Zhu, J., Li, C., Wong, D. F., & Chao, L. S. (2019). Learning deep transformer models for machine translation. arXiv preprint arXiv:1906.01787.

[37] Wang, X., Shen, Y., Wang, S., Li, S., Zhang, W., Liu, X., ... & Li, H. (2017). PharmMapper 2017 update: a web server for potential drug target identification with a comprehensive target pharmacophore database. Nucleic acids research, 45(W1), W356-W360.

[38] Wells, M. L., Trainer, V. L., Smayda, T. J., Karlson, B. S., Trick, C. G., Kudela, R. M., ... & Cochlan, W. P. (2015). Harmful algal blooms and climate change: Learning from the past and present to forecast the future. *Harmful algae*, *49*, 68-93.

[39] Weng, L. M., Su, X., & Wang, X. Q. (2021). Pain symptoms in patients with coronavirus disease (COVID-19): a literature review. Journal of Pain Research, 147-159.

[40] WHO. 2020. Coronavirus Disease (COVID-19) Advice for the Public: Myth Busters. Can Eating Garlic Help Prevent Infection with the New Coronavirus? https://www.who.int/images/default-source/health-topics/coronavirus/myth...

[41] Wu, F., Zhou, Y., Li, L., Shen, X., Chen, G., Wang, X., … Huang, Z. (2020). Computational Approaches in Preclinical Studies on Drug Discovery and Development. Frontiers in Chemistry, 8. doi:10.3389/fchem.2020.00726

[42] Zakharova, A. (2020). Chimera patterns in networks. Springer.

[43] Zheng, S., Fan, J., Yu, F., Feng, B., Lou, B., Zou, Q., ... & Liang, T. (2020). Viral load dynamics and disease severity in patients infected with SARS-CoV-2 in Zhejiang province, China, January-March 2020: retrospective cohort study. *bmj*, *369*.